

NASA TECHNICAL NOTE



NASA TN D-6585

2.1

NASA TN D-6585



LOAN COPY: RETU
AFWL (DOUL
KIRTLAND AFB, I

EFFECTS OF SURFACE CONTAMINATION
ON THE INFRARED EMISSIVITY
AND VISIBLE-LIGHT SCATTERING
OF HIGHLY REFLECTIVE SURFACES
AT CRYOGENIC TEMPERATURES

by Walter Viehmann and Alfred G. Eubanks

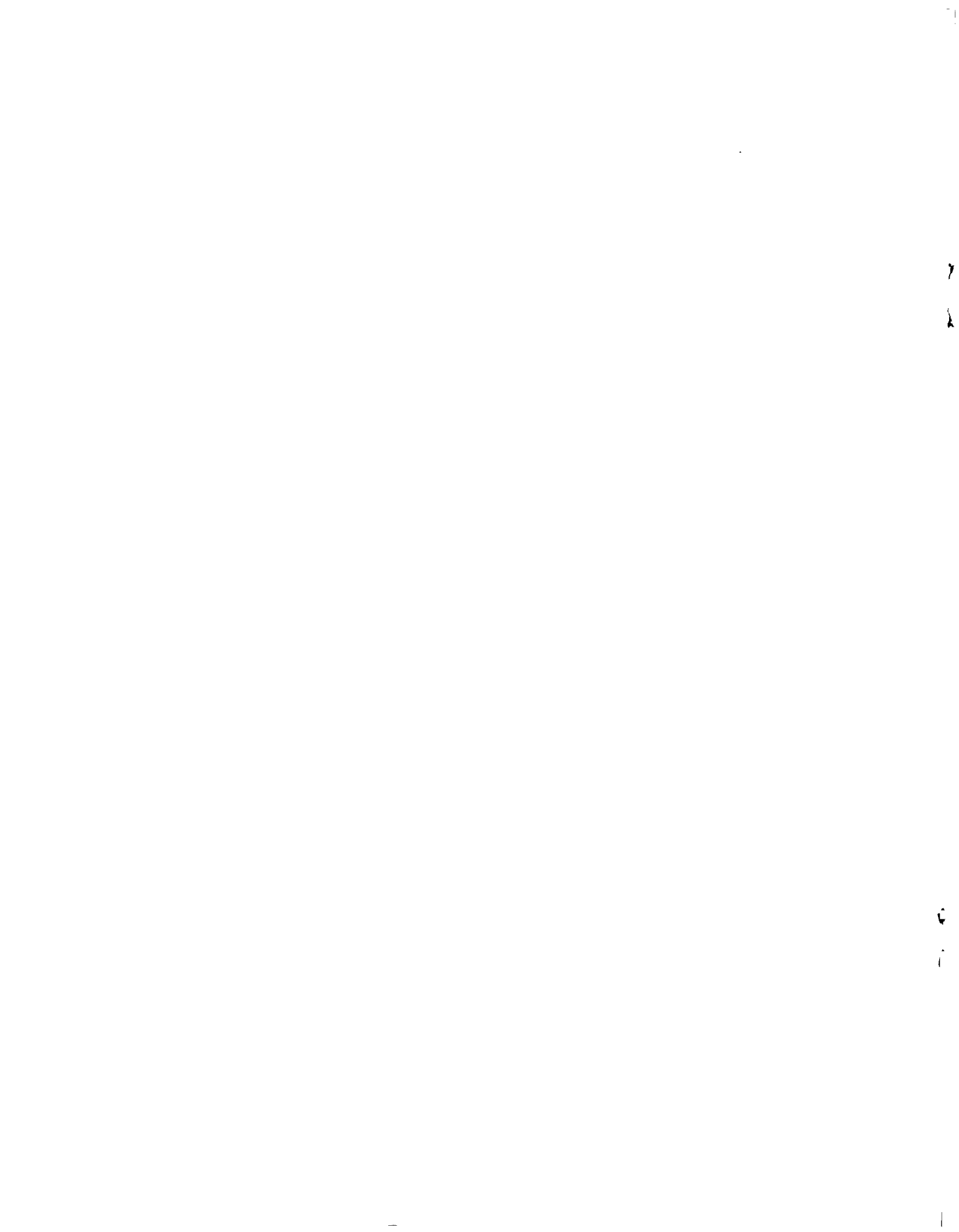
Goddard Space Flight Center

Greenbelt, Md. 20771



0133148

1. Report No. NASA TN D-6585		2. Government Accession No.		3. Recipient's Catalog No.	
4. Title and Subtitle Effects of Surface Contamination on the Infrared Emissivity and Visible-Light Scattering of Highly Reflective Surfaces at Cryogenic Temperatures		5. Report Date February 1972		6. Performing Organization Code	
7. Author(s) Walter Viehmann and Alfred G. Eubanks		8. Performing Organization Report No. G-1045		10. Work Unit No.	
9. Performing Organization Name and Address Goddard Space Flight Center Greenbelt, Maryland 20771		11. Contract or Grant No.		13. Type of Report and Period Covered Technical Note	
12. Sponsoring Agency Name and Address National Aeronautics and Space Administration Washington, D.C. 20546		14. Sponsoring Agency Code			
15. Supplementary Notes					
16. Abstract A technique is described for the simultaneous <i>in situ</i> measurement of film thickness, refractive index, total normal emissivity, visible-light scattering, and reflectance of contaminant films on a highly reflective liquid-nitrogen cooled, stainless steel substrate. Emissivities and scattering data are obtained for films of water, carbon dioxide, silicone oil, and a number of aromatic and aliphatic hydrocarbons as a function of film thickness between zero and 20 μm . Of the contaminants investigated, water has by far the greatest effect on emissivity, followed by silicone oil, aliphatic hydrocarbons, aromatic hydrocarbons, and carbon dioxide. The emissivity increases more rapidly with film thickness between zero and 2.5 μm than at thicknesses greater than 2.5 μm . Scattering of visible light changes very little below 2- μm thickness but increases rapidly with thickness beyond 2 to 3 μm . The effect of contaminant films on passive radiation coolers is discussed.					
17. Key Words Suggested by Author Contamination Emissivity Scattering Radiative Coolers			18. Distribution Statement Unclassified—Unlimited		
19. Security Classif. (of this report) Unclassified	20. Security Classif. (of this page) Unclassified	21. No. of Pages 12	22. Price \$3.00		



CONTENTS

	Page
Abstract	i
INTRODUCTION	1
EXPERIMENTAL TECHNIQUES AND MEASUREMENT PRINCIPLES	2
Instrumentation	2
Film Thickness and Refractive Index	3
Emissivity	4
RESULTS AND DISCUSSION	5
Infrared Emissivity Versus Film Thickness	5
Reflectivity and Scattering in the Visible Range	8
SUMMARY AND CONCLUSIONS	11
References	12

EFFECTS OF SURFACE CONTAMINATION ON THE INFRARED EMISSIVITY AND VISIBLE-LIGHT SCATTERING OF HIGHLY REFLECTIVE SURFACES AT CRYOGENIC TEMPERATURES

by

Walter Viehmann and Alfred G. Eubanks
Goddard Space Flight Center

INTRODUCTION

Infrared radiometers to be flown in a variety of satellite programs require cooled photodetectors operating in the 80- to 120-K temperature range. These temperatures are achieved by passive radiation cooling, i.e., by means of a "black patch" in radiative equilibrium with space. As a result of orbital, volume, and spacecraft-interface constraints, it becomes generally necessary to shield the patch against radiative energy inputs from the earth, the sun, and the spacecraft. The configuration of a typical cooler that has evolved under these constraints is illustrated in Figure 1. This design is usually referred to as a shielded two-stage cooler. The shield is at spacecraft temperature; the second, or detector, stage is at the photodetector operating temperature, and the first stage is at an intermediate temperature, typically 160 to 180 K. The internal cone surfaces are highly reflective specular surfaces having low emittance and absorptance in both the infrared and solar spectral regions in order to minimize earth and solar radiation absorption, as well as radiation transfer between stages.

Degradation of the optical properties of these surfaces is of great concern since a temperature rise in the detector stage will result. For instance, doubling the emissivity of the first-stage cone from 0.02 (which is typical of evaporated aluminum or gold) to 0.04 will cause an increase in the temperature of the detector stage by 5 to 10 K, depending on the particular cooler design (Reference 1). An increase of the nonspecular, or diffuse, component of the solar reflectivity will have a similarly detrimental effect.

Inasmuch as the first-stage cone is at low temperature, optical degradation as a result of condensation of contaminants (e.g., from such polymer outgassing products as low molecular weight solvents, water, and oils) is considered likely.

Quantitative data on the effect of contaminants on the infrared emissivity and visible-light scattering of specular surfaces at cryogenic temperatures are few. Caren, Gilcrest, and Zierman (Reference 2) measured the total hemispherical absorptance of water-vapor and carbon-dioxide deposits on polished aluminum and black-painted aluminum at 77 K for room-temperature blackbody radiation as a function

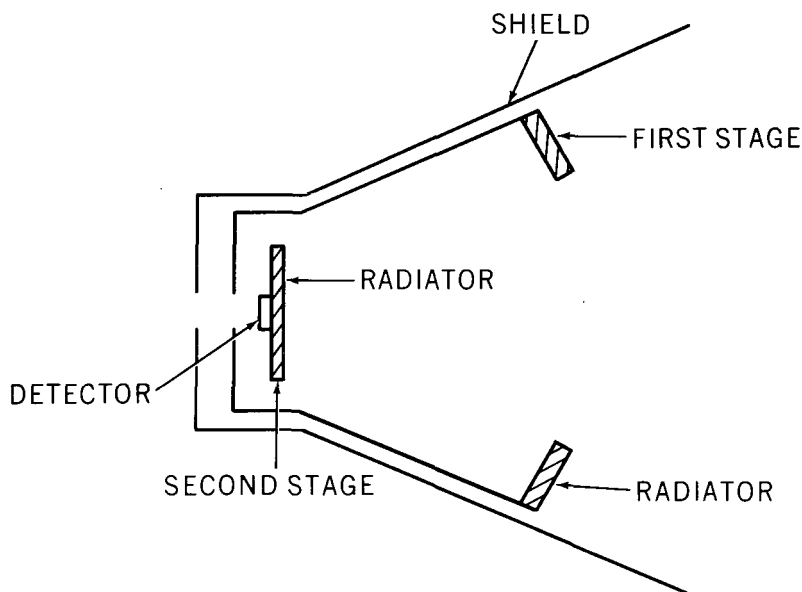


Figure 1—Schematic diagram of a shielded two-stage radiant cooler.

of thickness. Cunningham and Young (Reference 3) investigated the effects of carbon-dioxide condensation on polished copper and a black substrate.

In the present investigation, we have extended our measurements to thin films of model compounds that can be considered typical for outgassing products of satellites, satellite systems, and experiment packages.*

EXPERIMENTAL TECHNIQUES AND MEASUREMENT PRINCIPLES

Instrumentation

The experimental apparatus is designed such that film thickness, emittance, and scattering can be measured simultaneously during deposition of the contaminant film. A schematic diagram of the apparatus is shown in Figure 2. A polished stainless-steel substrate in the form of a hollow block of 8 cm X 6.6 cm X 3 cm (3 in. X 2.6 in. X 1 in.) external dimensions is located inside an evacuated bell jar and is cooled to 77 K by flowing liquid nitrogen. An He-Ne laser beam ($\lambda = 632.8$ nm), modulated at 500 Hz by means of a chopper, is split into two components by a beam splitter and directed onto the substrate at incident angles θ_1 and θ_2 . The intensities of the reflected beams are measured by silicon photodiodes, as is the intensity of scattered light at various angles θ_s . The reflected beams are polarized perpendicularly to the plane of incidence by means of the polarizers P . The signals from the diodes are fed to lock-in amplifiers, and the amplifier outputs are recorded by xy -recorders as a function of time while the films are being deposited. The total normal emittance of the films is measured

*J. C. Goldsmith, and E. R. Nelson, "Molecular Contamination in Environmental Testing at Goddard Space Flight Center", paper no. 2 presented at the ASTM/IES/AIAA Fifth Space Simulation Conference, Gaithersburg, Maryland, 1970.

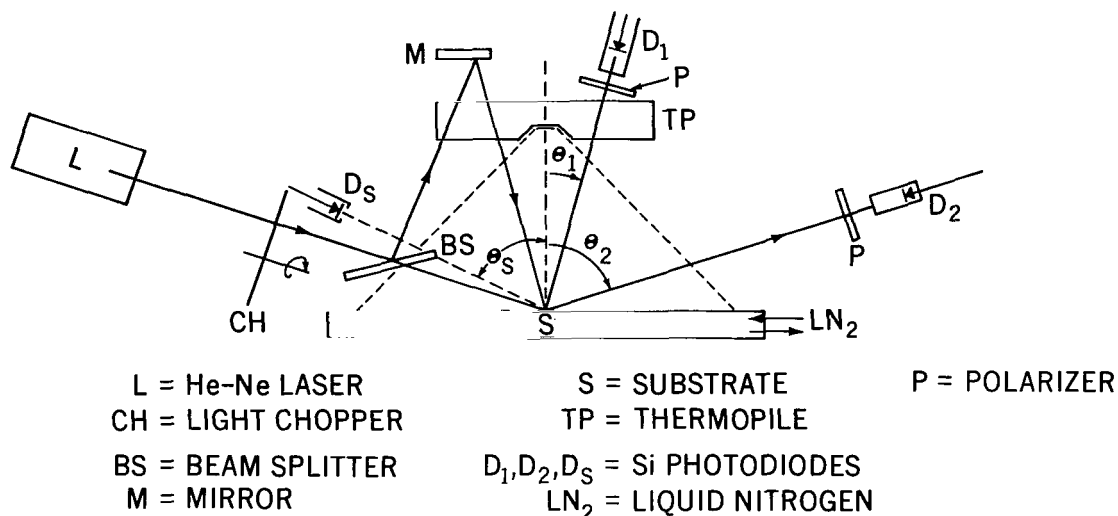


Figure 2—Schematic diagram of experimental setup for optical measurements of contaminant film.

by means of a thermopile, the output of which is amplified by a millimicrovoltmeter, and is also recorded as a function of time.

The pumping system consisted of a liquid-nitrogen trapped 10-cm (4-in.) diffusion pump backed by a mechanical pump. Pressures lower than 1×10^{-6} Torr could be routinely obtained. Formation of the films was achieved by introducing the various liquids or gases into the chamber through a controlled-leak valve. All films were grown under partial pressures less than or equal to 2×10^{-5} Torr, as measured by an ionization gauge connected to the base ring of the bell jar. Typical growth rates ranged from 100 to 500 nm per minute.

Film Thickness and Refractive Index

The measurement of film thickness is based on the occurrence of optical interference in transparent films.* Interference effects are observed in the reflected light as a result of the optical-path difference between the light reflected at the vacuum-film interface and that reflected at the film-substrate interface. This principle is illustrated in Figure 3. The optical-path difference Δ between the two reflected beams is determined by the angle of incidence θ_i , the thickness d , and the refractive index n of the film. If phase-shift corrections at the vacuum-film and film-substrate interfaces are neglected, the path difference is given by (Reference 4)

$$\Delta = 2d\sqrt{n^2 - \sin^2 \theta_i} . \tag{1a}$$

If this difference is $N\lambda$ and N is an integral number, the two beams will be in phase, resulting in constructive interference (reflectivity maxima), and if N is half integral, the two reflected beams will be 180 deg out of phase, resulting in destructive interference (reflectivity minima).

*For an example of a recent review of optical-thickness measurements, see Reference 4.

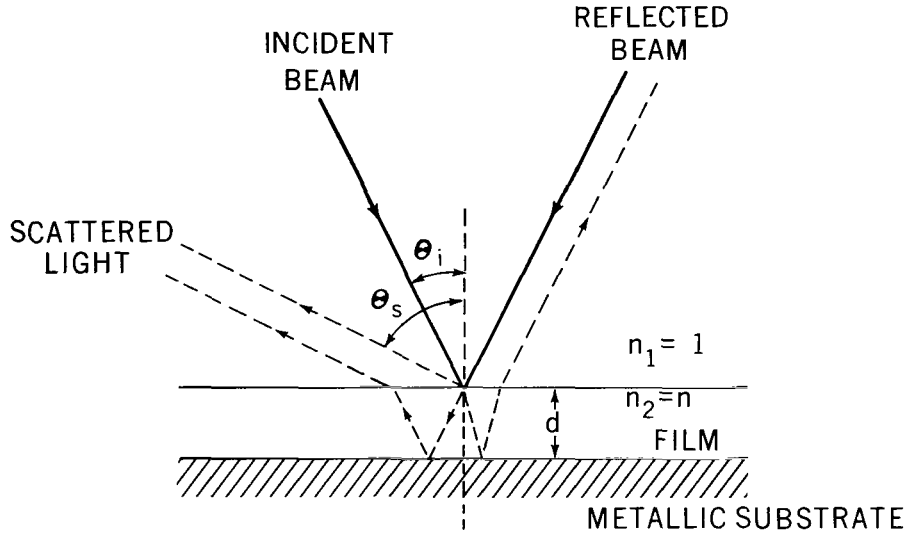


Figure 3—Schematic diagram of reflection and scattering from a transparent film on a metallic substrate.

Since reflectivity minima can be more accurately determined than maxima, film thicknesses are obtained from the relation

$$d = \frac{N\lambda}{2\sqrt{n^2 - \sin^2 \theta_i}}, \quad (1b)$$

where $N = \frac{1}{2}, \frac{3}{2}, \frac{5}{2}, \dots$ is the order of successive interference minima.

For accurate determination of d , the index of refraction of the film is required. Therefore, two simultaneous reflectivity measurements are made under two incident angles $\theta_1 = 30$ deg and $\theta_2 = 72$ deg, as was mentioned previously. From the number of minima N_1 and N_2 recorded at these angles for a given film thickness d , the index of refraction is determined from the relation

$$\frac{N_1 \lambda}{\sqrt{n^2 - \sin^2 \theta_1}} = \frac{N_2 \lambda}{\sqrt{n^2 - \sin^2 \theta_2}}. \quad (1c)$$

Emissivity

The difficulty of obtaining accurate emissivity values by radiometric methods is generally recognized (Reference 5), and certain precautions have to be taken to avoid serious errors in the results, particularly for low-emissivity values. In this work, we have chosen a comparison method; i.e., all values are measured relative to a blackbody of the same temperature as the sample. In order to create such a blackbody, the substrate was kept at 77 K and coated with a film of "frosty" ice of about 0.1-mm thickness. For this thickness, the emittance becomes independent of thickness, and e_n was taken to be 0.98, a value generally given in the literature for frosty ice (Reference 6).

The distance between thermopile and sample (substrate) is such that the latter fills the 60-deg field of view of the detector completely. If the detector, in thermal equilibrium with its surroundings, is set at zero signal output and a blackbody is then placed in its field of view, the resulting signal is (Reference 5)

$$S_{BB} = k(W_1 - \delta W), \quad (2a)$$

where k is a calibration constant, W_1 is the flux contributed by the blackbody, and δW is the fraction of the ambient flux W obscured by the blackbody. Similarly, for a nonblack sample of emissivity e_n , the signal becomes

$$S_s = k(e_n W_1 - \delta W + W_2), \quad (2b)$$

where $W_2 = R \delta W$ is the fraction of the ambient flux reflected by the sample. The ratio of the two signals thus becomes

$$\frac{S_s}{S_{BB}} = \frac{e_n W_1 + (R - 1) \delta W}{W_1 - \delta W}. \quad (2c)$$

Since the detector, having a field of view of 60 deg, admits only radiation within ± 30 deg of the normal, R can be approximated by $1 - e_n$, and the ratio becomes truly equal to e_n . However, because our sample and blackbody are at 77 K and ambient temperature is 300 K, W_1 and $e_n W_1$ are small compared with δW and $(R - 1) \delta W$, and the ratio S_s/S_{BB} becomes equal to $1 - R = e_n$ for 300-K blackbody radiation emanating from the surrounding bell jar, regardless of the validity of the above approximation.

RESULTS AND DISCUSSION

Infrared Emissivity Versus Film Thickness

Table 1 lists the compounds that were investigated and their indexes of refraction at $\lambda = 632.8$ nm as determined by the two-angle interference method described above. With these values, film thicknesses obtained from reflectance measurements in units of effective quarter wavelength were converted to physical thicknesses by use of Equation 1b.

Infrared absorption spectra of water, typical aliphatic hydrocarbons, silicone oil, and aromatic hydrocarbons are shown in Figure 4 (reproduced from commercial literature*). These spectra were measured at room temperature with a standard sample thickness of 10 μm , except for those marked with an asterisk, which were measured "between salts," i.e., with an unspecified thickness smaller than 10 μm . Qualitatively, therefore, it is apparent that water, aliphatic hydrocarbons, and silicone oil are strong absorbers of 300-K blackbody radiation. Absorption of aromatic hydrocarbons is weaker, and carbon dioxide (not shown in Figure 4) absorbs rather weakly only in the 4- to 5- μm band.**

*"26 Frequently Used Spectra for the Infrared Spectroscopist", Sadtler Research Laboratories, Inc., Philadelphia, Pa.

**B. E. Wood, A. M. Smith, B. A. Seiber, and J. A. Roux, "Spectral Absolute Reflectance Measurements of CO₂ Frosts in the 0.5 to 12.0 Micron Region", paper no. 41 presented at the ASTM/IES/AIAA Fifth Space Simulation Conference, Gaithersburg, Maryland, 1970.

Table 1—Compounds investigated and their indexes of refraction at $\lambda = 632.8$ nm and $T = 77$ K.

Material	Index of Refraction ($\lambda = 632.8$ nm)
Water	1.42
Acetone	1.36
Ethanol	1.36
Methanol	1.32
2-Propanol	1.33
Toluene	1.53
Silicone oil (DC-200)	1.36
Benzene	1.49
Trichloroethylene	1.48
Carbon dioxide	1.30

Figure 5 shows the total normal emissivity of the various contamination layers on polished stainless steel as a function of film thickness at 77 K.

In the early stages of film growth, i.e., between zero and approximately 2.5- μm thickness, emissivity increases rapidly with thickness. For carbon dioxide and benzene, e_n decreases slightly beyond 2.5 μm and goes through a minimum at about 4.5 μm before increasing further at a much slower rate with thickness. Maxima and minima in the emissivity-vs.-thickness curves are also observed more or less clearly in the other compounds. Since the separation between successive maxima or minima is about 4 to 5 μm , it seemed proper to

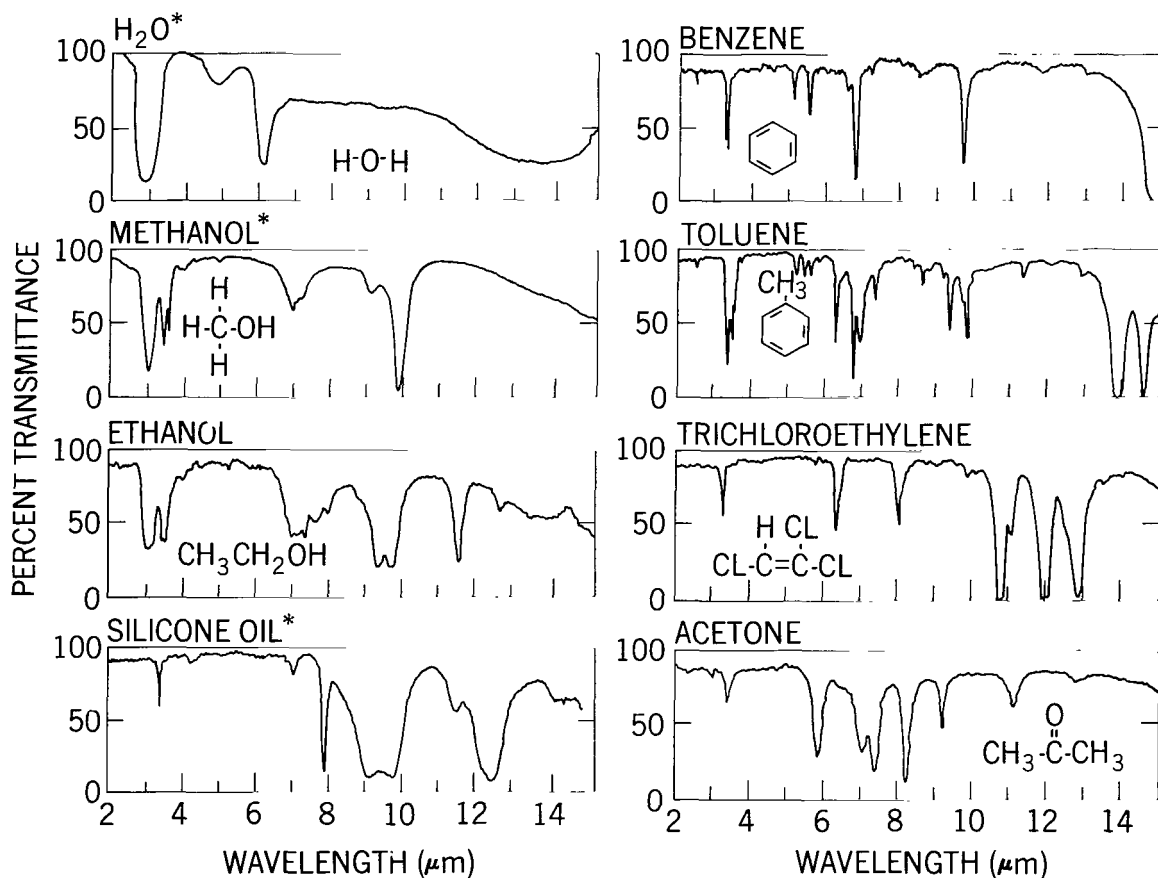


Figure 4—Infrared absorption spectra of water and some organic compounds. Measurements were made at room temperature with a sample of 10- μm thickness, except for those marked with an asterisk, which were made with a sample of unspecified thickness smaller than 10 μm .

interpret them as being due to interference effects in the reflection of the 300-K blackbody radiation, an altogether reasonable assumption in view of the discrete band structure of the infrared absorption of these compounds. In order to support this interpretation, monochromatic emissivity measurements were performed on a limited number of materials by placing an interference filter with a peak transmission wavelength of $10.8 \mu\text{m}$ and a bandwidth of $0.8 \mu\text{m}$ in front of the thermopile. The results are shown in Figure 6. Compounds that have little or no absorption in this spectral region show the interference maxima and minima very clearly. For ice, which is a strong absorber, only the first two minima can be observed.

From the point of view of contamination, it is important to note that ice has by far the greatest effect on the emissivity of a reflecting surface, particularly since water is believed to represent a significant fraction of the total weight loss caused by outgassing of polymeric materials. Also, multilayer insulation, which is frequently used for thermal-control blankets in general and in radiation-cooler construction in particular, outgasses copious amounts of water, with typical rates ranging from 10^{-6} Torr-liter-cm $^{-2}$ -s $^{-1}$ initially to 10^{-9} Torr-liter-cm $^{-2}$ -s $^{-1}$ after 15 hours in vacuum.*

At sufficiently large film thicknesses, i.e., for films of several micrometers thickness, the emissivities of the various compounds fall into relative ranges, which one might expect on the basis of their

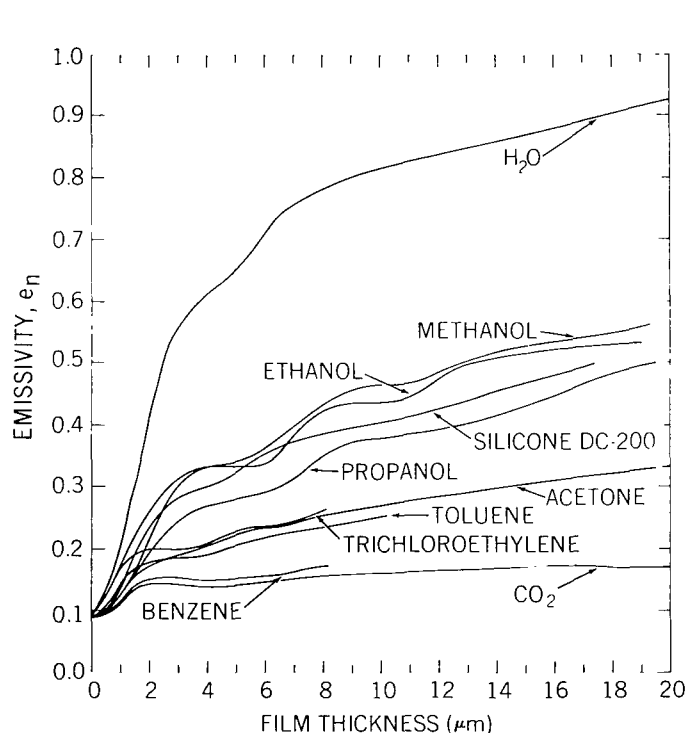


Figure 5—Emissivity as a function of film thickness on polished stainless steel at 77 K.

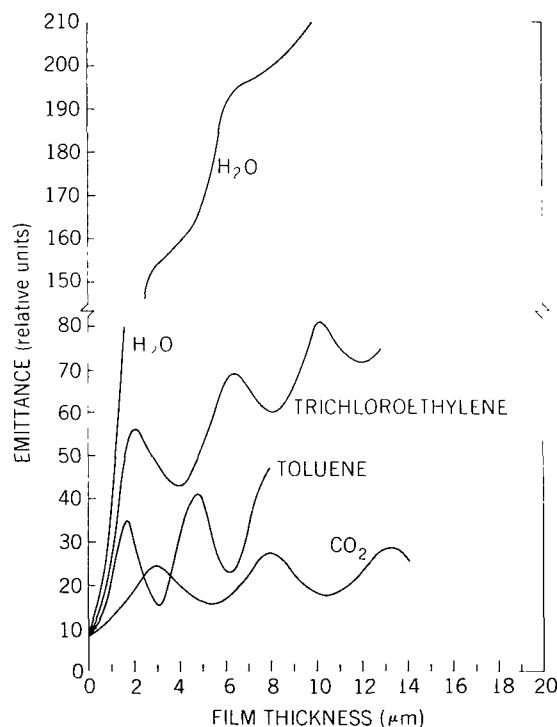


Figure 6—Emittance as a function of film thickness at $10.8 \pm 0.5 \mu\text{m}$.

*A. P. M. Glassford, in an unpublished report by the Lockheed Missile and Space Company, Palo Alto, Calif., NASA-Marshall Space Flight Center Contract No. Nas 9-20758.

infrared absorption spectra. Aliphatic hydrocarbons and silicone oils have significantly higher emissivities than the less-absorbing aromatic hydrocarbons, and carbon dioxide has the lowest emissivity of the materials investigated. It is important, however, to point out that for film thicknesses less than $2\ \mu\text{m}$, or roughly a quarter wavelength of 300-K blackbody radiation, no such straightforward relative ordering on the basis of absorption alone can be made. For this thickness range, emissivities are to a large degree determined by reflection losses, i.e., by the real part of the index of refraction around $10\text{-}\mu\text{m}$ wavelength. For instance, acetone, which is a relatively weak absorber in the infrared, has the same emissivity below $1\text{-}\mu\text{m}$ thickness as methanol and considerably higher emissivity than propanol and silicone oil, all of which absorb strongly in the infrared.

As was pointed out earlier, an increase in emissivity of the first-stage cone surfaces by about 0.02 results in significant degradation of performance for most radiant-cooler designs. It is apparent from Figure 5 that films of approximately 200-nm thickness of water or of about 1000 nm of carbon dioxide are sufficient to cause such an increase on a highly reflective surface. Values for the critical film thickness for organic contaminants fall in the 300- to 800-nm range, depending on their absorption coefficients and indexes of refraction in the $10\text{-}\mu\text{m}$ region of infrared radiation.

Reflectivity and Scattering in the Visible Range

Scattering measurements were made with an incident angle of $\theta_i = -72$ deg and a scattering angle of $\theta_s = -60$ deg (backscattering) into a solid angle of 10 deg. All intensities were normalized relative to that obtained with a perfectly diffuse sample of magnesium oxide in place of the substrate. A typical recording of reflected intensity and scattered intensity as functions of film thickness is shown in Figure 7. Maxima of reflected intensity occur when the effective film thickness

$$d_{\text{eff}} = d\sqrt{n^2 - \sin^2 \theta_i}$$

is an even number of quarter-wave multiples, and minima when the effective thickness is an odd number of quarter-wave multiples. The intensities of successive reflectance maxima and minima decrease due to absorption in the film. It is possible, in principle, to determine the complex index of refraction $n^* = n(1 + ik)$ (where k is the extinction coefficient) of the film from these reflectivity measurements by use of the proper Fresnel formulae (Reference 7) and by fitting measured reflectance data to computed curves. However, this is generally not done in practice, because the effects of scattering are difficult to take into account quantitatively. It has been shown experimentally by Hass and his coworkers (Reference 8) that scattering centers at the film surface affect the reflectance maxima very little and the reflectance minima very strongly. At reflectance minima, or effective odd quarter-wave thicknesses, the standing wave in the film has a loop at the surface that is strongly affected by absorbing layers or scattering centers; hence, the reflectance at minima changes more rapidly than at maxima, for which the electric field has a node at the surface of the film. Accordingly, interference minima of reflectance are accompanied by scattering maxima, and reflectance maxima by minima of scattered intensity.

In the early stages of film growth (i.e., between zero and about 10 quarter-wave thicknesses), the amplitudes of the scattering maxima increase very little with film thickness, as in Region I in Figure 7.

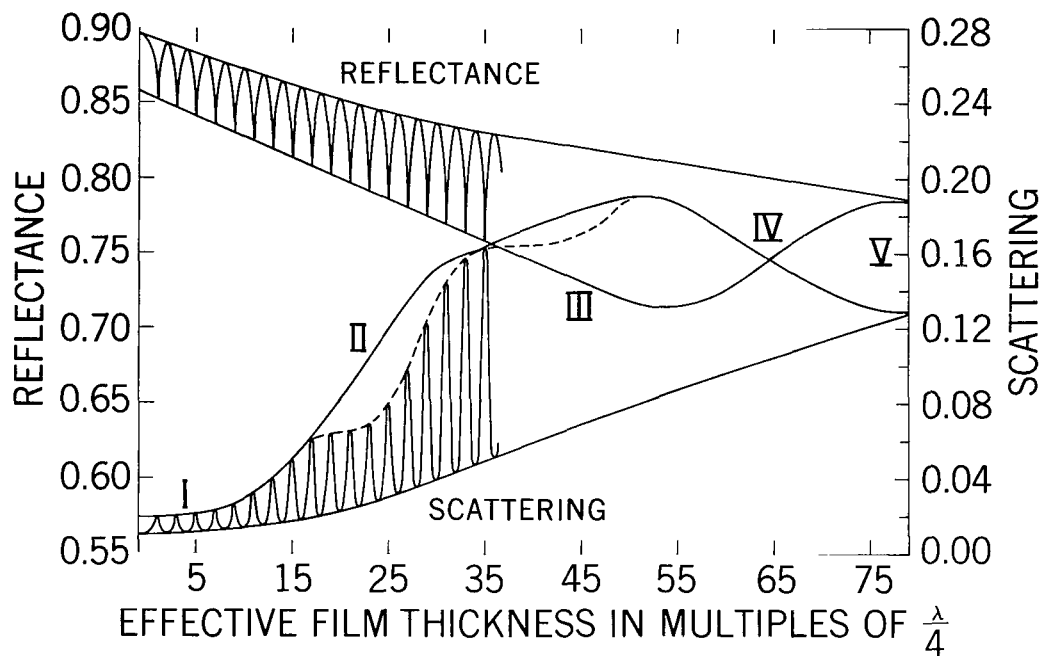


Figure 7—Reflected intensity and scattered intensity as a function of film thickness.

In this region, scattering is largely directional and is concentrated in a cone around the reflected beam. Backscattering is quite small compared to forward scattering.* Beyond a film thickness of about $2 \mu\text{m}$, the amplitudes of scattering maxima increase rapidly with thickness (Region II). During this period of growth, the angular distribution of scattering intensity changes from that characteristic of the substrate to that characteristic of the film, albeit still far from Lambertian. The films become hazy and visible to the naked eye during this period of growth, which extends to about 5 to $7 \mu\text{m}$ in most cases. Upon further increase in thickness, scattering maxima and minima increase at about the same rate (Region III). Eventually, the films become sufficiently diffuse to obscure interference effects in reflectance as well as scattering. Visually, they attain a frosty appearance. Interference maxima and minima of both reflectance and scattering wash out (Region IV) and finally converge into thickness-independent values characteristic of the diffusely scattering surface (Region V).

A somewhat puzzling feature of the scattering measurements is the occurrence of modulation of the scattering amplitude as a function of film thickness. This modulation was consistently observed in the course of these investigations. If one realizes, however, that an interference condition in the form of Equation 1a exists not only for the reflected beam, with $\theta = \theta_i$, but also for the scattered light, with $\theta = \theta_s \neq \theta_i$ (see Figure 3), and that the total hemispherical scattering intensity as a function of optical thickness is governed by θ_i and the angular intensity at an angle θ_s is governed by θ_s , it becomes apparent that the observed scattering amplitude is the "beat signal" resulting from the difference in optical path difference, $\Delta' = \Delta_i \pm \Delta_s$, between the specularly reflected beam (Δ_i) and the scattered beam (Δ_s).

*The angular distribution of scattering intensity as a function of film thickness is intended to be the subject of future investigations.

The resulting amplitude modulation of (angular) scattered intensity becomes particularly pronounced when this difference is deliberately made large. Figure 8 shows the amplitude modulation observed with $\theta_i = -5$ deg and two different scattering angles of -52 and $+10$ deg, respectively. A very pronounced modulation is seen for the scattering angle of -52 deg. For a viewing angle of 10 deg, on the other hand, the interference conditions for the total hemispherical scattering and angular scattering are sufficiently close to wash out any resulting modulation, since the solid angle of the detector is comparable to the difference in angle between the reflected beam and the scattered beam.

Figure 9 shows the results of the scattering measurements for the various compounds investigated. The above mentioned modulation effects are not shown. Each material is characterized by two curves: an upper curve for scattering maxima, which occur at odd multiples of effective quarter-wave thicknesses, and a lower curve for scattering minima, occurring at even multiples of quarter-wave thicknesses. The former is a measure of the surface scattering, and the latter of volume scattering and absorption in the films. For most compounds, surface scattering is significantly higher than volume scattering and absorption losses for thicknesses below about $20 \mu\text{m}$. Exceptions to this are benzene and carbon dioxide, which take on a frosty appearance from the beginning of film growth. Interference effects in films of benzene and carbon dioxide can be observed only for thicknesses below 7 and $10 \mu\text{m}$, respectively. In films of acetone and methanol, on the other hand, interference can be seen at thicknesses well beyond $20 \mu\text{m}$.

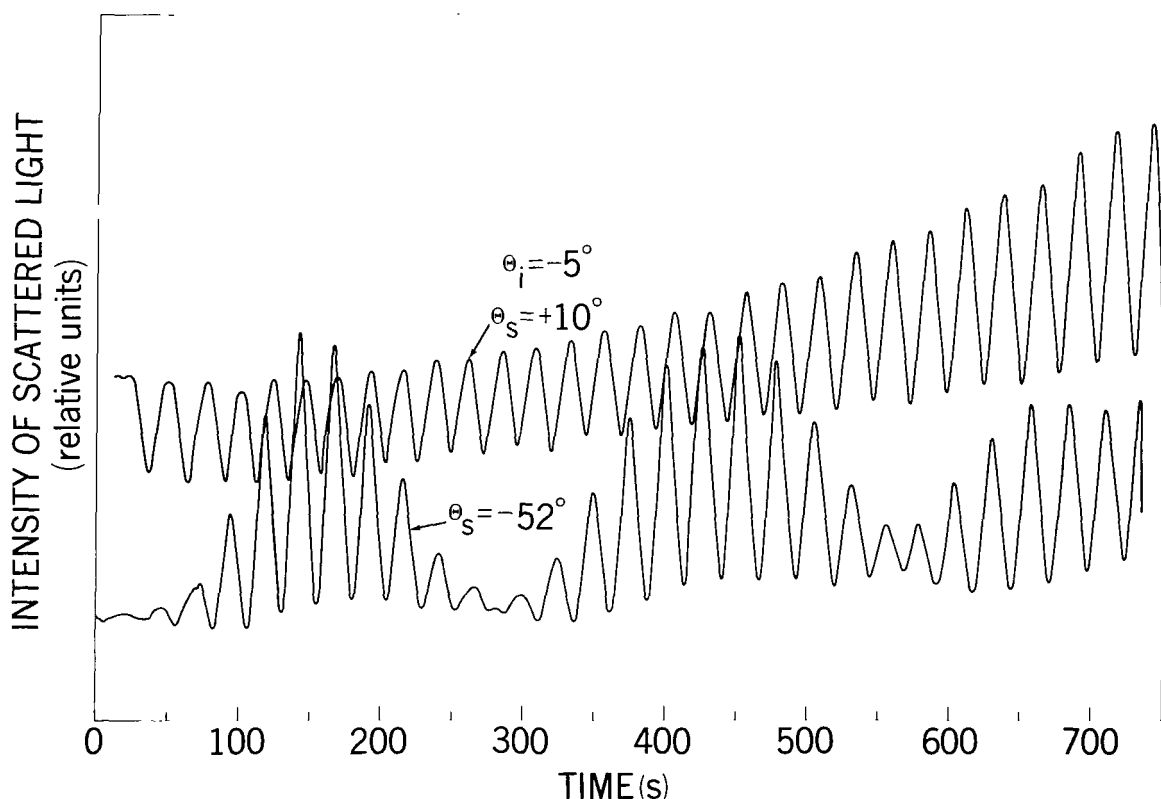


Figure 8—Modulation of scattering amplitude for two different relative angles of scattering.

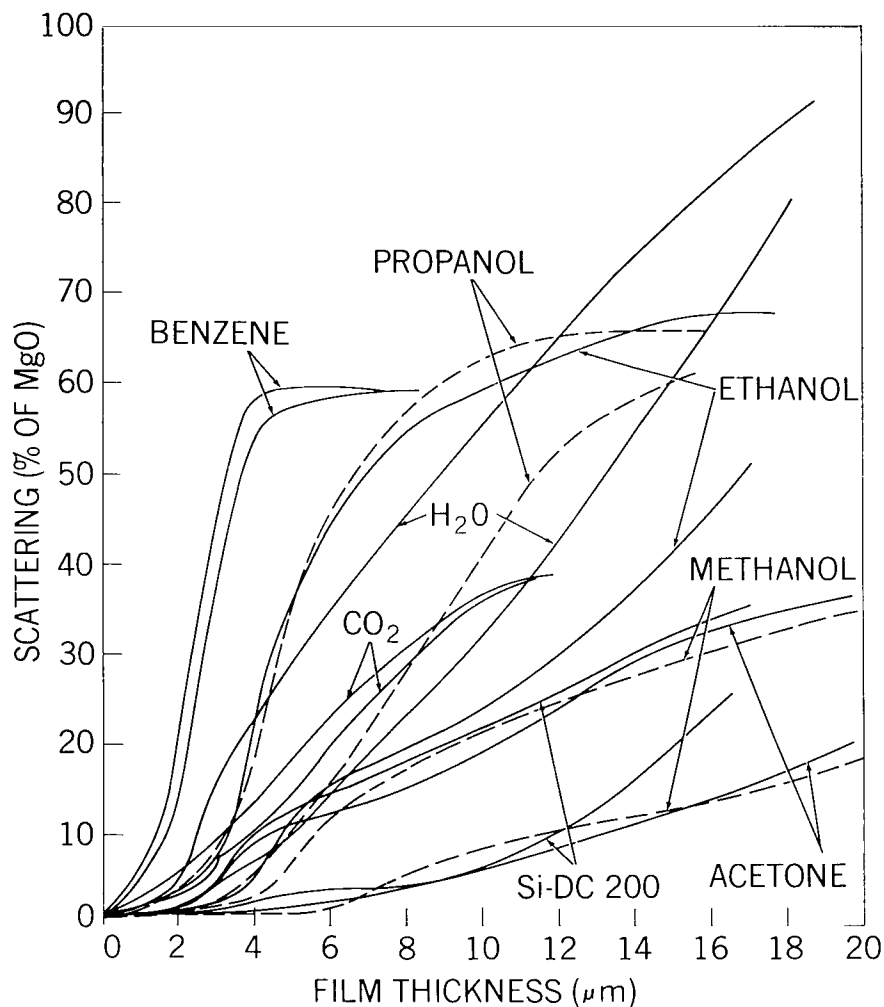


Figure 9—Scattering factor of contaminant films as a function of thickness at 632.8 nm, measured with an incident angle of -72 deg and a scattering angle of -60 deg. The upper curves are for odd-numbered multiples of $\lambda/4$, and the lower curves are for even-numbered multiples of $\lambda/4$.

The clean stainless steel substrate has a relative scattering factor of 1 percent of that for magnesium oxide. Except for benzene, films of 1.0- to 1.5- μm thickness will approximately double this value. Only beyond a thickness of about 2 μm does the scattering of typical films increase significantly. For thin films, therefore, the relative increase in scattering is small compared to changes in infrared emissivity.

SUMMARY AND CONCLUSIONS

Infrared emittance and visible-light scattering of highly reflective substrates are strongly affected by the deposition of contaminant layers. Emissivity increases most noticeably between zero and

approximately 2.5- μm thickness of the contaminant film as a result of reflection and absorption losses in the surface coating. In this thickness range, emissivity increase per unit film thickness is highest for water, followed in order by aliphatic hydrocarbons, silicone oil, aromatic hydrocarbons, and carbon dioxide. Scattering of visible light changes very little below about 2- μm thickness but increases rapidly with thickness beyond 2 to 3 μm . Shielded two-stage passive radiation coolers will be significantly degraded by the deposition of infrared absorbing contaminants of between 200- and 500-nm thickness.

Goddard Space Flight Center
National Aeronautics and Space Administration
Greenbelt, Maryland, July 21, 1971
821-21-78-01-51

REFERENCES

1. Annable, R. V., "Radiant Cooling", *Applied Optics* 9(1): 185-193, 1970.
2. Caren, P. R., Gilcrest, A. S., and Zierman, C. A., in *Advances in Cryogenic Engineering*, Plenum Publishing Corp., New York, 1964, Vol. 9, pp. 457-463.
3. Cunningham, T. M., and Young, R. L., in *Advances in Cryogenic Engineering*, Plenum Publishing Corp., New York, 1963, Vol. 8, pp. 85-92.
4. Pliskin, W. A., and Zanin, S. J., in *Handbook of Thin Film Technology*, L. I. Maissel and R. Glang, ed., McGraw-Hill Book Co., New York, 1970, Chapter 11.
5. Drummeter, L. F., and Hass, G., in *Physics of Thin Films*, G. Hass and R. E. Thun, ed., Academic Press, Inc., New York, 1964, Vol. 2, pp. 325-327.
6. Hudson, R. D., Jr., in *Infrared System Engineering*, John Wiley and Sons, New York, 1969, p. 44.
7. Heavens, O. S., in *Physics of Thin Films*, G. Hass and R. E. Thun, ed., Academic Press, Inc., New York, 1964, Vol. 2, p. 205.
8. Hass, G., and Hunter, W. R., "Laboratory Experiments to Study Surface Contamination and Degradation of Optical Coatings and Materials in Simulated Space Environments", *Applied Optics* 9: 2101, 1970.



010 001 C1 U 23 720121 S00903DS
DEPT OF THE AIR FORCE
AF WEAPONS LAB (AFSC)
TECH LIBRARY/WLOL/
ATTN: E LOU BOWMAN, CHIEF
KIRTLAND AFB NM 87117

POSTMASTER: If Undeliverable (Section 158
Postal Manual) Do Not Return

"The aeronautical and space activities of the United States shall be conducted so as to contribute . . . to the expansion of human knowledge of phenomena in the atmosphere and space. The Administration shall provide for the widest practicable and appropriate dissemination of information concerning its activities and the results thereof."

— NATIONAL AERONAUTICS AND SPACE ACT OF 1958

NASA SCIENTIFIC AND TECHNICAL PUBLICATIONS

TECHNICAL REPORTS: Scientific and technical information considered important, complete, and a lasting contribution to existing knowledge.

TECHNICAL NOTES: Information less broad in scope but nevertheless of importance as a contribution to existing knowledge.

TECHNICAL MEMORANDUMS: Information receiving limited distribution because of preliminary data, security classification, or other reasons.

CONTRACTOR REPORTS: Scientific and technical information generated under a NASA contract or grant and considered an important contribution to existing knowledge.

TECHNICAL TRANSLATIONS: Information published in a foreign language considered to merit NASA distribution in English.

SPECIAL PUBLICATIONS: Information derived from or of value to NASA activities. Publications include conference proceedings, monographs, data compilations, handbooks, sourcebooks, and special bibliographies.

TECHNOLOGY UTILIZATION PUBLICATIONS: Information on technology used by NASA that may be of particular interest in commercial and other non-aerospace applications. Publications include Tech Briefs, Technology Utilization Reports and Technology Surveys.

Details on the availability of these publications may be obtained from:

SCIENTIFIC AND TECHNICAL INFORMATION OFFICE

NATIONAL AERONAUTICS AND SPACE ADMINISTRATION

Washington, D.C. 20546